Available online at www.sciencedirect.com
SCIENCE DIRECT®
Microelectronic Engineering 77 (2005) 95–102
MICROELECTRONIC ENGINEERING
www.elsevier.com/locate/mee

Origins of debris and mitigation through a secondary RF plasma system for discharge-produced EUV sources

E. Vargas López *, B.E. Jurczyk, M.A. Jaworski, M.J. Neumann, D.N. Ruzic

Plasma-Material Interaction Group, University of Illinois at Urbana-Champaign, Physics, 103 S Goodwin Avenue, Urbana, IL 61801, USA

Received 9 April 2004; received in revised form 28 July 2004; accepted 1 September 2004
Available online 8 October 2004

Abstract

RF plasma based mitigation has been studied as an improved debris mitigation scheme for extreme ultraviolet (EUV) sources. The RF plasma ionizes sputtered neutral debris and, when used in conjunction with a collimator (also known as a foil trap), inhibits that debris from reaching the collector optics. An ionization fraction of 61 ± 3% has been measured. In addition, increased scattering of the ion component of the debris has led to a decrease in erosive flux reaching the diagnostics. Results from in situ high-precision quartz crystal oscillators, ex situ surface characterization (Auger, XPS), and secondary plasma characterization is presented for a series of mitigation schemes, including a foil trap in conjunction with the RF plasma.

Keywords: EUV; Debris mitigation; Lithography; Dense plasma focus; DPF; Secondary plasma; RF plasma; Ionization fraction

1. Introduction

Next generation extreme ultraviolet photolithography (EUVL) sources require several orders of magnitude improvement in the reduction of debris for component lifetime and to maintain stable operation [1]. Inductively coupled secondary plasma-based debris mitigation techniques for use on EUVL sources are described below. They are based on a concept pioneered by the iPVD reactors used in industry and here [2].

The *I*llinois *D*ebris-mitigation *E*UV *A*pplications *L*aboratory (IDEAL) consists of a dense plasma focus discharge source operating on the order of 15 J/pulse, 30 Hz rep rate, and 3 kV. Tests have been conducted with argon gas to generate plasma environmental conditions and debris profiles similar to that experienced in industry [3].

* Corresponding author. Tel.: 6306776520; fax: 2173332906.
E-mail address: vargaslo@uiuc.edu (E. Vargas López).

0167-9317/$ - see front matter
doi:10.1016/j.mee.2004.09.005

2. Theory

Consider a plasma source shown in Fig. 1. A dense pinch plasma is produced close to the anode of the source. During the pinch, energetic ions are created in the dense hot plasma and then move outward in all directions. A fraction of these ions strike the electrodes producing low-energy sputtered atoms. In addition, some of the ions incident on the electrodes reflect from the anode and cathode creating a source of medium-energy gas atoms. Another fraction of the highly energetic ions produced in the pinch travel the same path as the collected photons that are produced, and head straight toward the collector optics. This is not an exhaustive list of debris sources. Sudden heating of the electrodes can lead to atomic vaporization, ablation of molten material or other effects. All of these source terms are collectively referred to as 'debris'.

The collector optics lifetime problem arises because the sputtered electrode atoms accumulate on the mirror surfaces and decrease its reflectivity. Likewise, the energetic ions impinging on the surfaces will erode the mirror material. Surface roughening caused by these phenomena will ultimately degrade the mirrors if no mitigation scheme is in place.

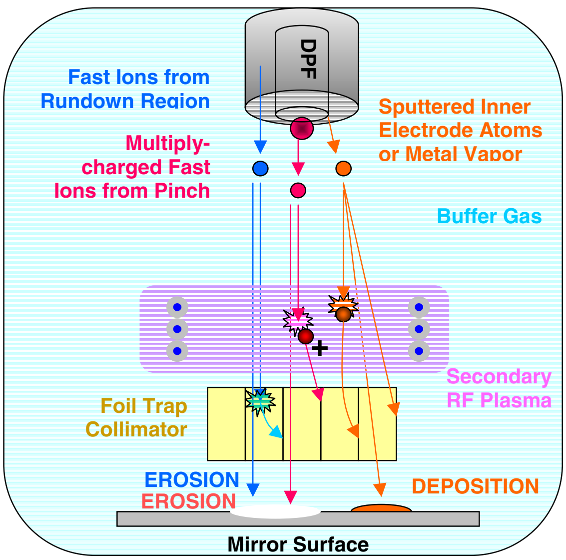

Fig. 1. The debris sources and their effect on the collector optics. The RF plasma and the foil trap combine to mitigate the debris and minimize erosion/deposition on the mirror surface.

2.1. Sputtered electrode debris

At high enough system pressures, such that the mean free path for a sputtered neutral atom is much less than the dimensions of the device, the sputtered electrode debris becomes a diffusive source. In our experiment, the center electrode is made of copper. The mean free path for sputtered atoms in a background gas has been the subject of numerous works [4,5]. Those calculations show that the mean-free-path, λ, for Cu in Ar can be given by

$$\lambda[\mathrm{cm}] = \frac{9.2}{P[\mathrm{mTorr}]}.$$

Typical DPF pressures are >15 mTorr. At these levels, the mean free path (<0.61 cm) is sufficiently small for the diffusion approximation to be valid.

2.2. Energetic ions

The energetic ions (and neutrals through charge-exchange) that arrive at the collector optics can be calculated to first order by simply looking at the uncollided flux after traveling a distance x. It is given by $I(x)$

$$I(x) = I(0)\exp\left(\frac{-x}{\lambda_{\mathrm{in}}}\right).$$

where $I(0) = I$, and is the mean-free-path for ion–neutral collisions. Charge exchange has a higher probability, but it does not change the direction of the particle nor its energy. The ion–neutral mean free path is given by

$$\lambda_{\mathrm{in}} = \frac{1}{n\sigma_{\mathrm{in}}},$$

where σ_{in} is the ion–neutral elastic scattering cross section and n is the gas density. The ion–neutral elastic scattering cross section has the value of about 3×10^{-16} cm^2 at 1 keV for Ar^+ in Ar [6,7]. Therefore for $P = 15$ mTorr, $\lambda_{\mathrm{in}} = 6.91$ cm. For $x = d = 15$ cm, $I(C_1) = 0.11\,I$ energetic ions or neutrals per pulse. Therefore, a significant fraction of the flux arrives at the collector optics uncollided and having experienced no loss of energy.

2.3. Mitigation schemes

In order to reduce the debris flux reaching the collector optics, collimators, also known as "foil traps", have been used. The mean free path of the debris particles plays a fundamental role in the effectiveness of the foil trap. If the mean free path is significantly shorter than the dimensions of the device, the source is diffusive and the foil trap is very effective. If the mean free path is very large, then the foil trap can only be as effective as its optical transmission, barring any electromagnetic effects or other mitigation schemes.

Although the foil trap reduces the amount of debris reaching the collector optics, extreme ultraviolet (EUV) sources still need order of magnitude improvements in debris mitigation to attain the lifetime required to make the technology economically feasible [1]. An improved mitigation scheme utilizes a secondary RF plasma in the region between the pinch and the foil trap. Consider Fig. 1. It shows a secondary plasma generated in the space between the source and the foil trap.

If there is no foil trap present, ions will diffuse in a similar manner to the neutrals. There will be no difference in the deposition rate compared to the gas-only case. What will change is the charge state of the flux arriving at the collector optics. The fast reflected neutral component will vanish and the fast ions will be attenuated as before. However, the ionization of the sputtered electrode debris allows the possibility of employing E/B repellers, such as a biased foil trap collimator.

The most efficient debris barrier, once a secondary ionization source is present, is the use of a foil trap collimator. Immersed in the plasma, the collimator will acquire a potential that is negative with respect to the plasma potential and serve as an ion sink. Essentially, all but the highest energy ions are blocked by the biased foil trap, so the goal is to ionize as much of the debris as possible. In addition, the RF plasma can reionize the charge-exchange neutrals which will then be driven toward the foil trap's induced bias. Ions can also scatter due to the presence of the plasma and will be Debye shielded.

A consideration for introducing a foil trap into an EUV source is to maximize its optical transmission so as to not inhibit the EUV photons from reaching the collector. In addition, the choice of material may become important if the performance of the EUV source turns the foil trap into an extra sputtering source. A solution may be to construct the foil trap out of the same material as the capping layer on the mirrors. In this way, damage to the mirrors would be minimized. Note, however, that sputtering would occur at the portion of the foil trap nearest the source. The sputtered particles then scatter and there is a possibility that they would re-stick to the foil trap before damaging the collector mirrors.

Another consideration is the physical construction of the foil trap. In order for the concept to be useful, the foil trap and secondary plasma source must be compatible with EUV source geometries. Although this is currently not well-defined and is ultimately source-specific, the distance from EUV source to the collector optics may be in the range of 15–20 cm. The debris mitigation scheme in IDEAL does not currently comply with this last restriction although an advanced model is in the works.

Finally, one must consider the possibility of the foil trap becoming saturated and losing efficiency. In this case, the foil trap would need to be cleaned or replaced. There is an effort in the community for low-cost disposable debris collectors that could serve as a cost-effective method for debris extraction. However, the source rate of debris is highly dependent on the EUV source conditions, plasma temperature, electrode loading, radiation exposure, material choice, active cooling, etc. The combination of debris collection with the minimization of generation effects leads to a potential cost-of-ownership model for a commercial EUV source.

3. Model

A debris model is developed from the three, distinct, phases of the pinch. The first is the rundown phase that creates a plasma gun effect. This causes a flux of high-energy ions to shoot out axially from the region between anode and cathode. Next, is the compression phase, which creates high-energy ions near the pinch region. Finally, the pinch phase creates high-energy ions at the pinch whose distribution is isotropic in the expanding plasma. In the compression and pinch phases, the anode is bombarded with high-energy ions and will sputtered Cu from the anode that contributes to the debris. The mean free path of Cu in Ar is significantly smaller than the dimensions of the chamber for typical operating pressures, so the Cu source is assumed to be diffusive.

The RF plasma causes a fraction of the debris to ionize. The parameters that control the ionization fraction include plasma density and plasma temperature. The more dense the plasma becomes, the shorter the mean free path for ionizing particles becomes and the more likely that a particle will become ionized before reaching the QCM crystal. Likewise, a higher plasma temperature provides more ionization events by increasing the number of high-energy ionizing particles. Adjustable settings for the secondary plasma configuration that control the plasma parameters include: RF power, frequency, gas flow rate, pump rate, and a matching pi network for optimization. However, the plasma parameters in IDEAL are currently limited by sputtering of the coil. This becomes irrelevant if a foil trap is put in place to intercept this debris as well. In addition, several techniques have been developed to optimize the setup in IDEAL [3].

Experimental data for debris measurements is taken by use of the quartz crystal monitors. The quartz crystals oscillate at their natural frequency until a change in mass affects the oscillations. The change in mass can be due to debris being deposited on the crystal or high-energy particles eroding the crystal surface. In the IDEAL setup, a dual set of crystals is employed with one crystal being covered and acting as an in situ reference crystal. The dual nature of the QCMs allows extremely sensitive measurements to be made by removing differences due to thermal fluctuations or other inconsistencies [8]. Therefore, the differences of the crystals' frequencies allow us to monitor the relative mass deposition on the crystal. In the graphs, a positive slope means that there is net mass deposited on the QCM. The geometry of the chamber, as well as the placement of the diagnostics allows consistent assumptions to be made about the debris flux incident on the QCMs. For the case where the crystals are directly underneath the anode, the debris flux is due to the high-energy ions from the compression and pinch phases, in addition to the sputtered Cu flux. If the foil trap is in place, the flux of ions is unchanged because their trajectories are assumed to be straight lines within the dimensions of the chamber. However, the amount of sputtered Cu is reduced by an optical transmission factor as well as the ionized fraction from the secondary plasma.

By moving the QCM off axis, the ions from the rundown phase become visible to the diagnostic. Now, the debris is due to these ions, as well as those corresponding to the compression and pinch phases. The same amount of sputtered Cu debris will reach the QCM due to its diffusive nature. The addition of a foil trap affects the sputtered Cu debris by the same reduction factor as in the on axis case, while it completely eliminates the pinch phase ions by eliminating the line of sight path to the QCM. The model is summarized in the Table 1.

Table 1
Each of the debris components contribute independently to the total debris marked 'QCM Slope'

	On axis		Off axis	
	No FT	FT	No FT	FT
Background	+0.048	+0.007	+0.223	+0.042
Sputtered Cu	X	$(1-i)\alpha X$	X	$(1-i)\alpha X$
Rundown Ions	0	0	Y	Y
Pinch Region Ions	Z	Z	γZ	0
QCM Slope	+1.70	−1.39	−0.182	−0.790

α(0.828) is the transmittance for a diffusive source.
γ(0.928) is a geometrical reduction factor for oblique incidence when the QCM is off axis.

4. Experiment

Silicon witness plates were placed in the chamber near the crystal monitors throughout >100,000 shots for typical operational settings.

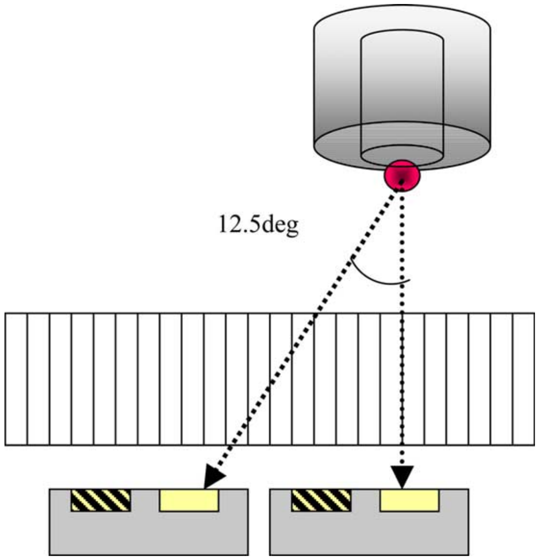

Fig. 2. On and off axis placement of the QCM allows isolation of the debris sources. Note that off axis, the line of sight ions are blocked by the foil trap.

These were later analyzed by Auger spectroscopy and X-ray photoelectron spectroscopy to verify the deposition of debris. Auger spectroscopy results affirm that the anode material is in fact being sputtered while the cathode is not. Meanwhile, XPS results show implanted Ar in silicon witness plates. This is a testament to the presence of high-energy ions in the debris field.

To quantitatively measure the amount of debris produced, multiple data runs were conducted on and off axis (~12.5° from the pinch) as shown in Fig. 2. Background measurements are taken that account for the contribution due to the presence of the secondary plasma as well as a general tendency for the crystal frequencies to vary. Another background measurement is taken with the foil trap in place. Finally, the dense plasma focus is operated both with and without the foil trap in place. These eight data points allow for a systematic analysis and provide a self-consistent model of the debris mechanisms.

For a diffusive source, as corresponds to the sputtered Cu debris, the transmittance of sputtered electrode material that goes through the foil trap can be calculated. For a cylindrical hole, as in Fig. 3, the top sees a diffusive distribution of debris

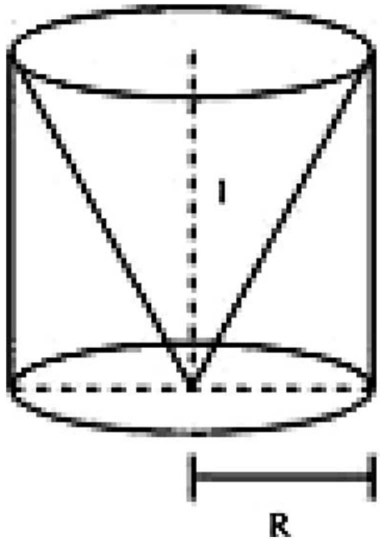

Fig. 3. The transmittance of a cylindrical hole is dependent on its aspect ratio. This quantity is (l/2R) as labeled here.

for 2π steradians. However, a point at the center of the bottom sees only a cone of height l and width 2R for a solid angle

$$\int_0^{2\pi}\int_0^{\tan^{-1}R/l}\sin\theta\,\mathrm{d}\theta\,\mathrm{d}\phi = 2\pi\left(1-\cos\left[\tan^{-1}(R/l)\right]\right) = 2\pi\left(1-\frac{l}{\sqrt{l^2+R^2}}\right).$$

As the Cu diffuses through the cylinder, only that fraction will reach the other side of the foil trap. The foil trap in IDEAL consists of 19 such cylindrical holes arranged in a circular pattern with $l = 2$ in. and $R = 0.219$ in. for an aspect ratio of 4.6. For these experiments, it was placed 2 in. above the QCM, and therefore, diffusive flux from the sides must also be accounted for. For the geometry in IDEAL, the transmittance of a diffusive source was calculated to be 0.828. This means that 82.8% of the sputtered electrode flux will make it to the QCM. It is so high because of the 2 in. spacing between the bottom of the collimator and the QCM.

The optical transmission of the foil trap refers to the amount of photons that are unobstructed as they traverse the foil trap. This will also roughly correspond to the transmission of the high energy ions as there are assumed to follow straight-line trajectories. Viewed from the QCM directly underneath the pinch, the optical transmission is 100%. This reflects the fact that the foil trap is wider than the QCM crystal, and therefore does not inhibit high-energy ions or photons from reaching the QCM. When the QCM is in its off axis position, the dimensions of the foil trap do not allow any light to reach the QCM and the optical transmission becomes 0% as shown in Fig. 2. This takes into account the dimensions and placement of the diagnostic and foil trap. Our group's previous work in iPVD provides a more in-depth look at calculation of transmittance for various aspect ratios [9].

Each of the data points was taken for at least 20 min. This is the amount of time for which transient behavior dies off in the system and there is constant deposition or erosion on the QCM. Therefore, each of the four stages of the data runs contributes to this total in a steady state manner as well if they act independently. Preliminary assumptions are the types of debris present for each rundown and pinch. In Table 1, the shaded regions are experimentally measured quantities.

Experimental values for the table correspond to the slope of QCM data at that setting. This experimental data set was taken with an RF power ~15 W. Langmuir probe measurements of n_e and T_e have been inconclusive due to high electromagnetic noise despite shielding of the components and installing RF filters. Fig. 4 shows those data points corresponding the row marked "QCM Slope." Error bars on all slope measurements are ~10%.

The system of equations ($X + 0 + Z = 1.65$, etc.) can be solved for each debris component, and the ionization fraction is determined from here as well. The factor of α is the optical transmission of the foil trap for a diffusive source. The factor of γ is a geometrical reduction factor that accounts for the pinch region ions at oblique incidence to the QCM surface. Both α and γ are calculated geometrically. i is the ionization fraction of the sputtered Cu. In our case, α is calculated to be ~0.828, and γ is ~0.928.

Solving the system of equations yields the following values for X, Y, Z, and i:

Sputtered Cu flux (X) = 4.48.
Rundown Ions (Y) = −2.26.
Pinch Region Ions (Z) = −2.82.
Ionization Fraction (i) = 0.61 ± 0.03.

Note that the Cu flux is largest contribution to the debris. However, by using a foil trap that intercepts 2π steradians, this flux would significantly decrease to <0.05 due to the transmittance. This

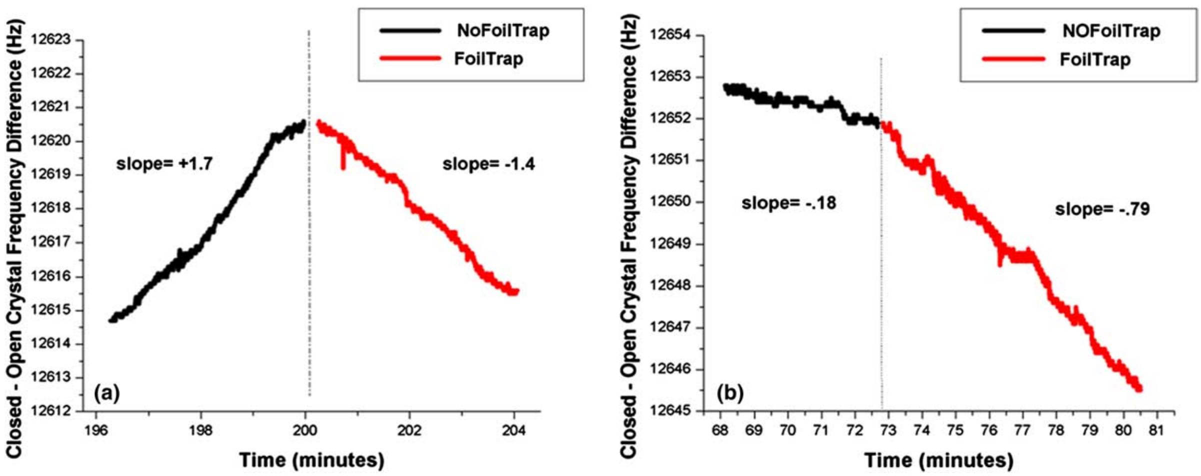

Fig. 4. These graphs correspond to the data points labeled 'QCM Slope' In each case, the DPF pulses with and without the foil trap: (a) on axis; (b) off axis.

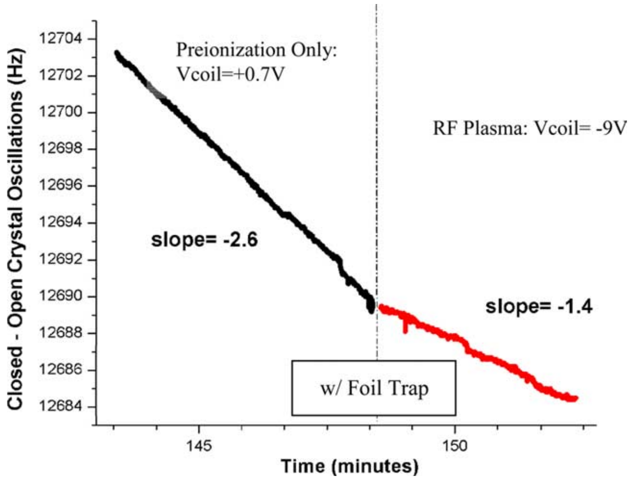

Fig. 5. Pulsing with preionization only then turning the RF plasma on results in less erosion to the QCM. Increased coulomb scattering is responsible for a decrease in the number of high-energy ions incident on the surface.

is consistent with observations in commercial devices that energetic ions are the main sources of mirror degradation [1].

Separate data points were taken with RF power ∼0 W. The purpose is to provide the preionization for the breakdown to occur, while not ionizing the

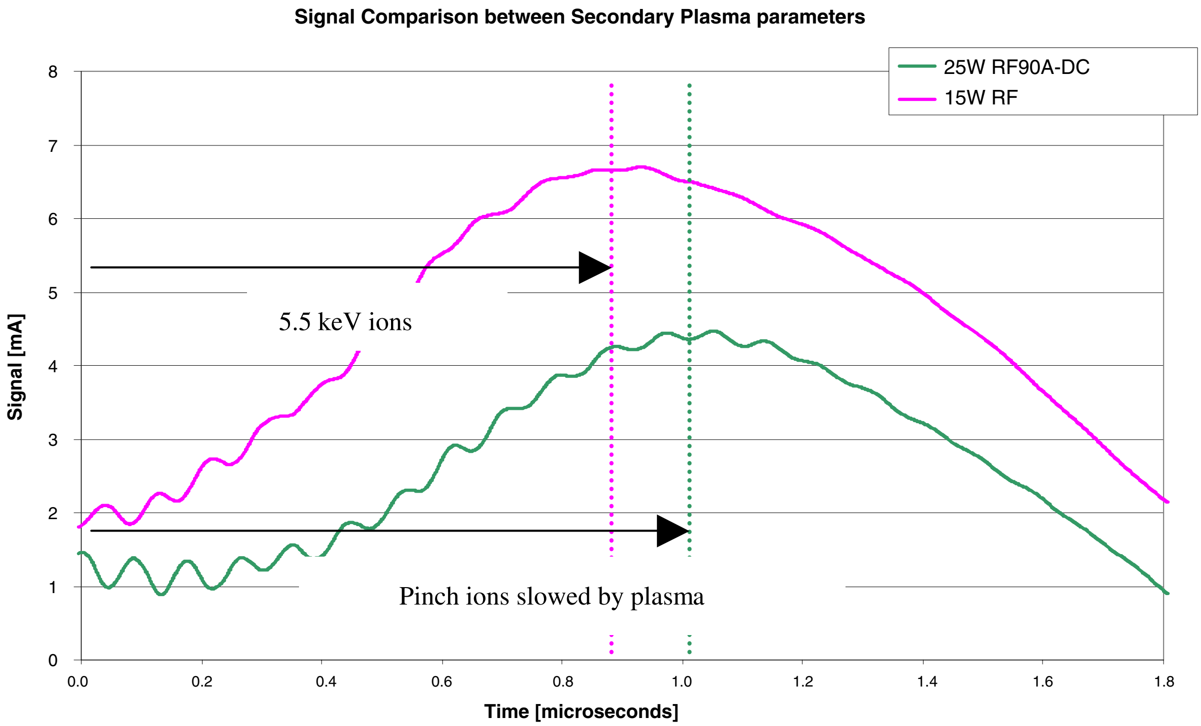

Fig. 6. The ion collector grid shows a decrease in the ion signal when the RF plasma is present. In addition, the ions are observed to slow down by the plasma.

sputtered Cu debris. Fig. 5 shows that turning on the RF plasma decreases the erosion to the QCM.

Further evidence comes from mounting an ion collector grid in the chamber below the DPF. The grid shows that as the RF input power is increased, the ion signal goes down and the ions slow down as well. Fig. 6 shows this phenomenon. In one case the plasma in the chamber is sustained by 15 W input power. The second case involves a much denser plasma and more confined in the region between the foil trap and the pinch. 25 W of RF power is input into the device with the addition of 90 Amps of DC current through the helicon antenna. These operating conditions yield a plasma with $n_e = 10^{11}$ with a temperature of a few eV's. Although the low power Langmuir probe measurements were inconclusive, visual inspection shows a much more intense discharge in the antenna region.

Time of flight analysis of the measurements shows a reduced ion signal amplitude as well as reduced mean energy. This indicates that some screening of fast ions is occurring by merely having a secondary RF plasma in the chamber. This comes about through increased coulomb scattering. The mean free path decreases with increasing number density. In addition to this, the bulk of the high-energy ions are the same species as the secondary RF source plasma is, resulting in the largest possible energy transfer during collision events. Both of these effects could account for the reduced ion signal measured on the ion collector grid.

5. Summary

Component lifetime is an important consideration for the viability of EUV sources and mitigating debris is vital for increasing it. IDEAL has shown to successfully mitigate debris. Experimental measurements indicate approximately 60% ionized sputtered electrode debris for RF-enhanced debris mitigation for very low power plasmas (<15 W). In commercial devices, this amounts to an increase in optics protection factor. In addition, IDEAL has also showed an influence on fast ion mitigation by the RF plasma. The result is encouraging as RF plasmas with higher n_e, T_e will improve the degree of ionization. Previous experience [4,9] leads us to believe that at 35 mTorr of Ar we will be able to sustain a $T_e = 2.5$ eV plasma with an electron density of 3×10^{11} cm^{-3}. This will lead to an ionization fraction of >90% for the sputtered neutral flux [5].

The next steps will be to improve the helical resonator immersed coil with Faraday shielding to allow higher power and densities with minimal capacitive coupling and sputtering of the coil. In addition, collaboration with source suppliers is an ongoing venture in which the ideas will continue to be developed, and the design adapted for commercial device specifications.

Acknowledgements

This work was performed under a research grant from INTEL Corp. # SRA 03–159.

A portion of the work was carried out in the Center for Microanalysis of Materials, University of Illinois, which is partially supported by the U.S. Department of Energy under grant DEFG02-91-ER45439.

References

[1] Available from: http://www.sematech.org/resources/litho/meetings/euvl/20021014/14-Debris.pdf, to be published in the SPIE Proceedings, Santa Clara, 2004.
[2] D.B. Hayden, D.R. Juliano, M.N. Neumann, M.M. Allain, D.N. Ruzic, Surf. Coat. Tech. 121 (1999) 401–404.
[3] B.E. Jurczyk, E. Vargas Lopez, M.J. Neumann, D.N. Ruzic, in: Proceedings of SPIE Microlithography Conference, Santa Clara, February 2004.
[4] D.R. Juliano, D.N. Ruzic, M.M.C. Allain, D.B. Hayden, J. Appl. Phys. 91 (2002) 605–612.
[5] D.R. Juliano, Modeling and measurements of an ionized physical vapor deposition device plasma, PhD Thesis, Department of Physics, University of Illinois at Urbana-Champaign, Advisor: D.N. Ruzic, 2000.
[6] D.N. Ruzic, S. Cohen, J. Chem. Phys. 83 (1985) 5527–5530.
[7] M.A. Lieberman, A.J. Lichtenberg, Principles of Plasma Discharges and Materials Processing, John Wiley & Sons, New York, 1994.
[8] J.P. Allain, D.N. Ruzic, Nucl. Fusion 42 (2002) 202–210.
[9] K.M. Green, D.B. Hayden, D.R. Juliano, D.N. Ruzic, Rev. Sci. Instrum. 68 (1997) 4555–4560.